Ordered Polyelectrolyte "Multilayers". 3. Complexing Clay Platelets with Polycations of Varying Structure

K. Glinel,[†,‡] A. Laschewsky,[‡] and A. M. Jonas*[,†]

Unité de physique et de chimie des hauts polymères, Université catholique de Louvain, Place Croix du Sud, 1, B-1348 Louvain-la-Neuve, Belgium (European Union), and Département de chimie, Université catholique de Louvain, Place Louis Pasteur, 1, B-1348 Louvain-la-Neuve, Belgium (European Union)

Received January 22, 2001; Revised Manuscript Received May 3, 2001

ABSTRACT: Different poly(ammonium) salts with various chemical structures were self-assembled by the layer-by-layer method with a synthetic hectorite, Laponite. Using X-ray reflectometry, we show that internal order is present in all multilayers. The structure of the polycation slightly modulates the spatial extent of order in the film as well as the value of the repeat period which increases with the volume per charge of macromolecule. By combining XRR, XPS, and TGA results, we demonstrate that the internal order in multilayers is due to the regular intercalation of organic polymer between individual platelets of Laponite and not due to the presence of nonexfoliated particules. This conclusion is corroborated by a structural analysis of the bulk complex between Laponite and a poly(diallylammonium) salt.

Introduction

The fabrication of polyelectrolyte multilayers via electrostatic self-assembly (ESA) has been widely studied for surface modification. It is one of the simplest and most cost-effective methods for preparing thin films.[1,2] However, the method is limited by the extensive interpenetration between neighboring "layers" leading to a low degree of internal order.[1−5] Currently, the preparation of stable and internally ordered multilayer films by ESA remains a challenge, although there is an increasing interest in the development of well-organized nanostructured films, to design advanced electronic, electrochemical, catalytic, or optical devices. Different routes for obtaining well-organized multilayer films have been explored. Recently, we reported that the use of lyotropic ionenes combined with proper polyanions leads to ordered electrostatic self-assemblies.[6] Unfortunately, these results have been restricted to few examples up to now. Another approach consisting of the sequential adsorption of two-dimensional inorganic anionic nanoparticles and polycations was recently explored to obtain ordered multilayers. The high surface area of such platelets allows to minimize layer interpenetration. So, various multilayers were prepared with different nanoparticles including platelets of metal oxides,[7−9] metal phosphates,[10−17] metal disulfides,[18,19] polyoxometalates,[20−23] graphite oxides,[24−28] perovskite,[29] and clay.[30−40] However, in most cases, no evidence for structural internal order was reported. Exceptionally, the sequential adsorption of polycations and clay platelets has attracted a wide interest because of the presence of a Bragg reflection testifying for some degree of internal organization of the films.[30,32−33,37,39]

Regrettably, most studies[30−40] describing electrostatic self-assemblies of clays with polycations used a narrow set of commercial polyelectrolytes like poly(diallyldimethylammonium chloride) (PDDA), poly(ethylene imine) (PEI), poly(2-vinylpyridine), or poly(4-vinylmethylpyridinium) as polycation components. Because of this, the understanding of polycation/clay complex organization remains limited. In fact, most previous studies on the structure of multilayers made from delaminated clay and a polycation[30−34,37,39] have been restricted to PDDA (polymer **1**, Figure 1) as polycation. In all cases, the presence of a Bragg peak corresponding to a repeat period of 14 ± 0.5 Å was reported, but different explanations were proposed for its presence. Kleinfeld and Ferguson[30−33] assumed that this repeat period corresponds to the repetition of polymer/clay layers with the polycation being intercalated between individual sheets of clay to form an ordered structure. By contrast, Kotov and co-workers[37] attributed this Bragg peak to the interplatelet basal spacing of the pure clay. They argued that no polymer intercalates between platelets since the value of repeat period (14 Å) is quite similar to that found for the basal spacing in hydrated sheets of pure montmorillonite. Accordingly, these authors proposed a structural model according to which undelaminated stacks of montmorillonite platelets are interlaced with polymer layers. To select among these two models, we investigated the influence of the chemical structure of the polycation employed on the multilayer structure. Here, we report on multilayers obtained from structurally very different polycations as shown in Figure 1. All these polycations bear quaternary ammonium groups that are known to complex well with clays.[41] Polycations with a relatively stiff main chain (**1** and **2**) as well as with a flexible main chain (**3**−**5**) were employed. Polymers **1** (used as reference) and **2** are closely related, with the positive charge located on the cycle in the backbone. However, the presence of the additional pyrrolidinium ring in **2** increases the stiffness of the chain. Ionene **3** also bears the positive charges on the backbone, with additional mesogenic hydrophobic side groups inducing a lyotropic behavior for this polycation.[42] When combined with the proper polyanion, ionene **3** leads to ordered self-assemblies.[42] By contrast, in the polymethacrylates **4** and **5**, the cationic groups are placed at the end of flexible side chain spacers of differing lengths (C_2 and C_{11}, respectively). The long hydrophobic spacer confers polysoap characteristics to

[†] Unité de physique et de chimie des hauts polymères.
[‡] Département de chimie.

10.1021/ma010123j CCC: $20.00
Published on Web 06/19/2001

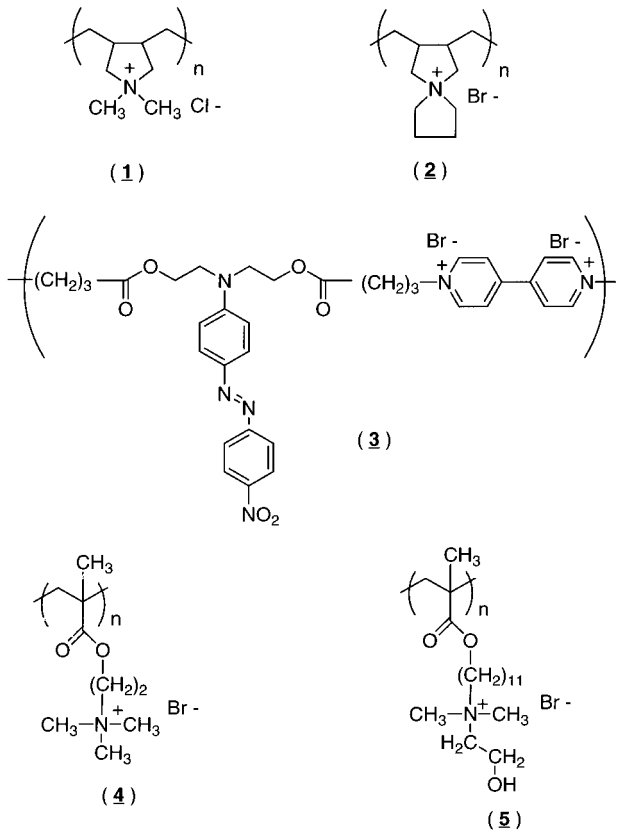

Figure 1. Chemical structure of the polycations used in this study.

5 and enables the formation of lyotropic liquid crystalline phases in concentrated water solutions.[43]

All these polycations were combined with a simple synthetic hectorite, Laponite. By contrast with natural clays, the chemical composition and the shape of platelets of such synthetic smectites are well-defined. Moreover, Laponite is easy to delaminate in individual particles in aqueous solution. A previous study[34] showed that higher coverages can be obtained with Laponite compared to other natural clays.

Experimental Section

A. Materials. 1. Polycations. Poly(diallyldimethylammonium chloride) (PDDA) (**1**) was purchased from Aldrich and used without purification. Commercial PDDA is known to be branched;[44] however, as shown by others,[45] branching does not affect multilayer growth and thickness. Poly(diallylpyrrolidinium) bromide **2**, ionene bromide **3**, and polymethacrylates **4** and **5** were synthesized as described elsewhere.[46−49]

2. Clay. Laponite clay (60% SiO_2, 29% MgO, 0.9% Li_2O, 2.9% Na_2O; 9.8% weight loss on ignition) from Laporte Industry was a gift from Chimilab Essor (La Madeleine, France). The chemical structure of this synthetic clay is analogous to hectorite. Silicate sheets are negatively charged, and the anionic sites are balanced by sodium cations. Platelets are approximately disk-shaped with an average diameter of 300 ± 100 Å (measured by transmission electron microscopy) and with a thickness of 9.2 Å.

3. Substrate. One-side polished ⟨100⟩ silicon wafers from ACM (France) were cut into rectangles of 3 cm × 1 cm. They were first cleaned by treatment with hot piranha solution [H_2O_2 (27%):H_2SO_4 (98%) 1:1 v/v] for 20 min *(caution: piranha solution is extremely corrosive)* and then thoroughly washed with purified water (Millipore, resistance = 18.2 MΩ).

B. Preparation of Multilayers. 1. Polycation Solutions. The polycations were dissolved in purified water with a concentration of 10^{-2} M (by repeat unit). The solutions were filtered through a 0.45 μm Millipore filter unit.

2. Clay Suspension. A 0.25 g sample of Laponite was dispersed under stirring in 100 mL of deionized water. This suspension was vigorously stirred at 6000 rpm for 12 h and then filtered through a 0.45 μm Millipore filter unit to remove aggregates of particles. A freshly prepared suspension was always used for self-assembly.

3. Multilayers Buildup. Multilayers were assembled by alternatively dipping the substrate in the solution of the polycation and in the suspension of Laponite for 10 min each. After each dip into either solution, the substrate was rinsed by immersion into three beakers with pure water and dried by a stream of hot air. These operations were repeated to obtain multilayers. All multilayers were terminated by a Laponite as topmost layer. Multilayers made of n cycles of polycation A and Laponite will be shown as $\{A/Laponite\}_n$ in the following.

4. Polyelectrolyte Complexes. The bulk hybrid complex was obtained by mixing the polycation solution and Laponite suspension used for the preparation of multilayers under vigorous stirring. The precipitate was collected by centrifugation at 10 000 rpm. A 0.2 g sample of the complex was stirred in 50 mL of water for 1 h and then separated by centrifugation at 10 000 rpm. This washing process was repeated three times to remove uncomplexed material.

C. Characterization Techniques. 1. Thermogravimetric analysis (TGA) was performed with a TGA-7 thermal analysis system (Perkin-Elmer) under a nitrogen atmosphere (30 mL min^{-1}) with a heating rate of 20 °C min^{-1}.

2. Ellipsometry. Ellipsometric data were obtained with a Digisel rotating compensator ellipsometer from Jobin-Yvon/Sofie Instruments working at 6328 Å wavelength (He−Ne laser). Measurements were performed at a fixed incident angle of 70°. To compensate for some systematic errors (imperfections and residual misalignement of optical components), each data point was obtained by averaging the results of two measurements with the analyzer successively set to +45° and −45° (with respect to the plane of incidence).[50] For each sample, between six and eight spots were measured and averaged. In all cases, film thickness was checked to be homogeneous all over the sample. A model consisting of an isotropic film on a flat substrate was used to fit the Ψ and Δ measurements.[51] The refractive index of silicon was taken to be 3.882-j0.019.[52] The effective refractive index of the film was obtained from ellipsometric data by fitting trajectories in the (Ψ, Δ) plane corresponding to samples of increasing thickness. Typically, a refractive index of 1.47 would be obtained by this procedure. The presence of a native oxide layer atop the silicon substrate does not influence the refractive index but results in an overestimation of the film thickness by about 15 Å.

3. Small-Angle X-ray Scattering. SAXS measurements were performed in transmission in a dried helium atmosphere with a Kratky compact camera mounted on a Siemens rotating anode (Ni-filtered Cu Kα radiation (λ = 1.5418 Å), 40 kV/300 mA). A calibrated position-sensitive proportional counter (mBraun) was used to record the scattering patterns. Details of the experimental procedure are described in ref 6. SAXS intensities are reported vs the length of the scattering vector, $s = (2/\lambda) \sin \theta$, where λ is the X-ray wavelength and θ is half the angle between incident and scattered beams.

4. X-ray Reflectometry (XRR). The experimental setup is based on a Siemens D5000 2-circles goniometer. X-rays of 1.5418 Å wavelength (Cu Kα) were obtained from a rotating anode. Monochromatization was achieved with the help of a secondary graphite monochromator, complemented with pulse height discrimination (scintillation counter). Proper collimation of the beam was obtained by using slits adjustable with micrometer precision. More information on the experimental setup can be found in ref 6. The corrected intensity is reported vs K_{z0}, the component perpendicular to the interface of the wavevector in a vacuum of the incident photons (i.e., $K_{z0} = (2\pi/\lambda) \sin \theta$, where λ is the X-ray wavelength and θ is half the angle between the incident and reflected beams). Data analysis was performed either by Fourier transforming the data after

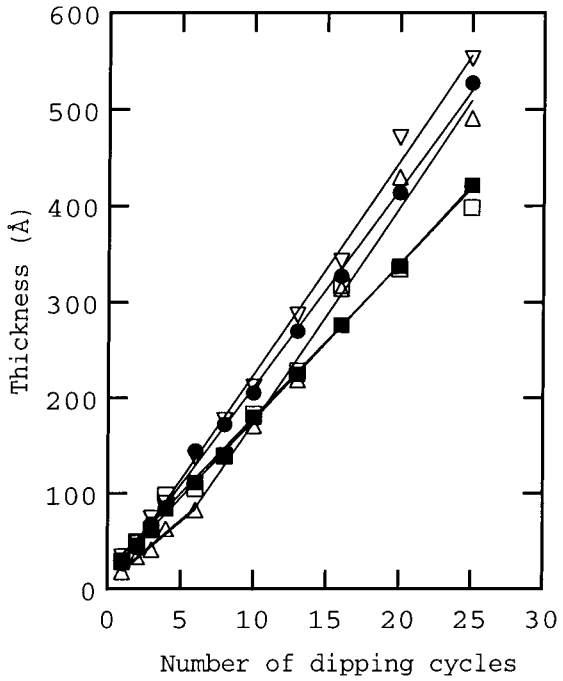

Figure 2. Variation of sample thickness vs number of deposition cycles for multilayers Si/{polycation/Laponite} prepared with various polycations: (□) **1**, (●) **2**, (△) **3,** (■) **4**, (▽) **5**. The lines are fits to the data.

proper normalization to obtain Patterson function or by fitting the data by standard routines, as described previously.[6]

5. X-ray Photoelectron Spectroscopy (XPS). X-ray photoelectron spectra were obtained using an Scienta ESCA 300 spectrometer. Measurements were performed with an Al Kα line source ($h\nu$ = 1486 eV) and with a pass energy of 75 eV and a resolution of 0.6 eV. The typical operating pressure was 10^{-10} Torr. The calibration was performed by referring the C 1s to the binding energy at 284.6 eV. The samples were measured at 30° and 90° takeoff angles (with respect to the plane of surface). The quantitative analysis of surface composition was obtained by integration of several scans for each individual element. Estimated errors on elemental composition are about 0.5%.[53,54]

6. Electron Dispersive X-ray Microanalysis (EDX). Microanalyses were performed using an energy-dispersive X-ray system (EDAX Phoenix equipped with a CDU LEAP detector) linked to a field effect gun scanning electron microscope (DSM 982 Gemini from Leo).

Results

Film Growth. The buildup of the films was monitored by ellipsometry. The variation of film thickness with the number of dipping cycles is given in Figure 2. For samples prepared with polycations **1**, **2**, **4**, and **5**, thickness increases linearly with number of dipping cycles, indicating a regular film growth over all the range of deposition cycles studied. For the system {**3**/Laponite}, the growth increment evolves over the six first adsorption cycles before reaching a constant value. A similar behavior was previously described in the literature for organic multilayers built with different polyelectrolyte pairs. This effect probably results from the perturbing influence of the substrate.[55] The increment per cycle depends only slightly on the nature of the polycation, varying between 16 and 22 Å per cycle for **4** and **3** or **5**, respectively (Table 1).

Influence of the Polycation Used on the Film Structure. XRR experiments were performed in order to investigate the internal structure of multilayers.

Table 1. Structural Data from XRR and Ellipsometry on Si/{Polycation/Laponite}$_n$ Multilayers

polycation	thickness increment per cycle[a] (Å/cycle)	repeat distance, d (Å)[b]	thickness of polycation layer[c] (Å)	ratio R[d]
1	17 ± 0.5	14.4 ± 0.5	5.2 ± 0.5	1.18
2	21 ± 0.5	14.4 ± 0.5	5.2 ± 0.5	1.46
3	22 ± 0.5			
4	16 ± 0.5	15.7 ± 0.5	6.5 ± 0.5	1.02
5	22 ± 0.5	17.5 ± 0.5	8.3 ± 0.5	1.26

[a] From ellipsometric measurements by linear regression. [b] From XRR measurements. [c] Value extracted from the repeat distance in accordance with eq 1. [d] Ratio between increment of thickness per cycle and repeat distance.

Measurements for self-assembled films with three dipping cycles are presented in Figure 3a. For all samples, only a single Kiessig fringe corresponding to the film thickness is seen at low angles, which points to an important roughness of the film/air interface. The most interesting feature of these reflectograms is the presence of a broad Bragg peak, indicating the presence of limited internal order in the films. These peaks can be better observed by plotting the reflectivity divided by the Fresnel reflectivity of the bare substrate (Figure 3b). Internal order is also clearly revealed by oscillations in Patterson functions calculated from these reflectograms (Figure 3c). The spatial extent of these oscillations depends slightly on the polycation used. Only for **1** and **2**, the vertical correlations extend over the total film thickness (∼45 Å) determined by ellipsometry. For the other polycations, regular oscillations are limited to a distance of about 30 Å. In all cases, the amplitude of the oscillations decreases rapidly with distance. This indicates that the self-assembled films are only partially ordered, with only restricted variations of order being observed following polycation nature. This observation is confirmed by an analysis of electron density profiles computed from the reflectivity curves (Figure 3d). Regions with larger electron density can be attributed to positions of the clay platelets and regions with smaller electron density to positions of organic polymer interlayers. For all samples, a large peak corresponding to the first well-organized layer of clay platelets is clearly observed close to the substrate. However, the following peaks broaden and decrease strongly in height, indicating a loss of periodic character with increasing distance from the substrate. This increasing disorder also leads to an important roughness of film/air interface, as testified by the large tailing of the electron density profiles. Clearly, {polycation/Laponite}$_n$ multilayers are well-ordered only over the first layers near the substrate.

Inspection of Figure 3b shows that the position of Bragg peaks depends on the polycation used. The repeat periods (d) extracted from Bragg peak positions are listed in Table 1. Values vary from 14.4 to 17.5 Å going from polycation **1** to **5**. It was not possible to determine precisely the repeat period for samples prepared with **3**, due to the low intensity of the Bragg peak.

The influence of the nature of the polycation appears more clearly when considering the thickness (p) of the organic polymer layers, calculated from the repeat period d by taking into account that each individual clay platelet provides a 9.2 Å thick spacer between polycation layers:

$$p = d - 9.2 \quad (\text{Å}) \qquad (1)$$

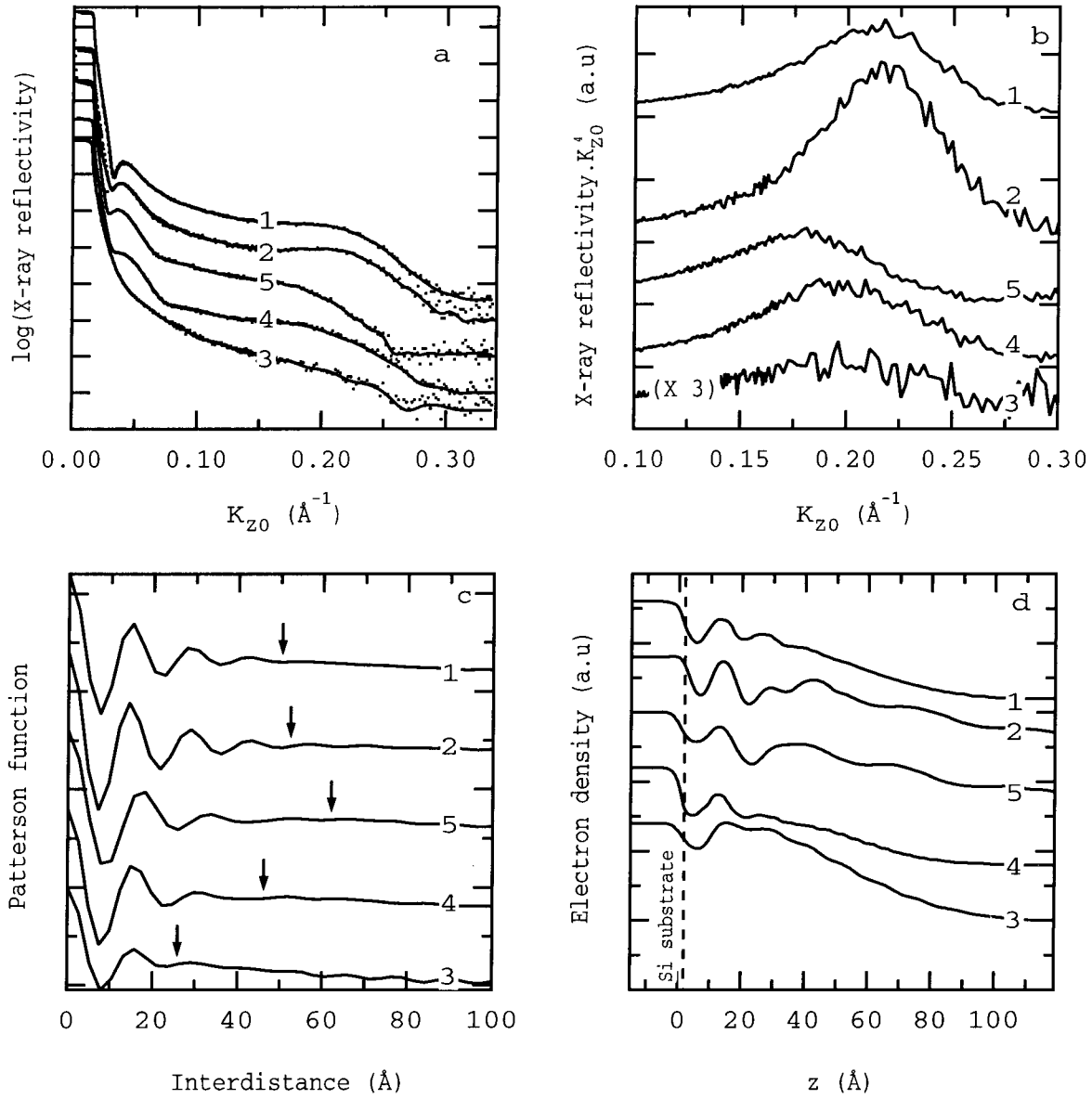

Figure 3. (a) X-ray reflectivity of Si/{polycation/Laponite}$_3$ multilayers prepared with different polycations (for numbering, refer to Figure 1). Curves are displaced vertically for clarity. Dots: experimental data. Continuous line: fits using the density profiles presented in (d). (b) X-ray reflectivity of same samples with intensities multiplied by K_{z0}^4 for a better view of Bragg peak. Curves are displaced vertically for clarity. (c) Patterson functions of the same samples. Vertical arrows indicate the film thickness. (The thickness of the native silicon oxide layer (15 Å) was subtracted from the total thickness measured by ellipsometry.) Curves are displaced vertically for clarity. (d) Electron density profiles obtained from the model-free fits to the experimental reflectivity. Curves are displaced vertically for clarity.

The thickness p of each polymer layer as given in Table 1 increases from 5.2 to 8.3 Å going from polycation **1** to **5**. The comparison of the increments of thickness per cycle with the repeat periods also gives clues about the mechanism of film growth. The ratio R between the increment of thickness per deposition cycle (determined by ellipsometry) and the repeat period d is listed in Table 1. For all samples, the ratio R is equal to or larger than 1, indicating that each adsorption cycle corresponds to the deposition of 1−2 monolayers of clay platelets.

Influence of Temperature on Film Structure. The clear dependence of the position of the Bragg peak on the chemical structure of the polycation strongly suggests that complete exfoliation of the clay particles occurs and that the polycation intercalates between each platelet. To verify this conclusion, we investigated the variation of the structural characteristics of {**2**/Laponite}$_n$ multilayers following various thermal treatments. Two samples with 10 dipping cycles were heated respectively to 180 °C under vacuum for 1 h and to 550 °C in an ambient atmosphere for 30 min. These samples were then directly introduced in a closed cell filled with an atmosphere of dry argon. The results of the XRR measurements in dry argon are displayed in Figure 4. The reflectogram of the initial multilayer in ambient air is shown for comparison (curve c). No significant difference can be seen between the film in air and the film measured in dry argon after the heat treatment at 180 °C: The position of the Bragg peak remains constant. We therefore conclude that the internal structure of multilayer is not modified by drying. By contrast, a decrease of the magnitude of the Bragg peak as well as a shift to larger angles shows up after heating the sample to 550 °C. A repeat period of 11.3 Å is determined which corresponds to the basal spacing of dried

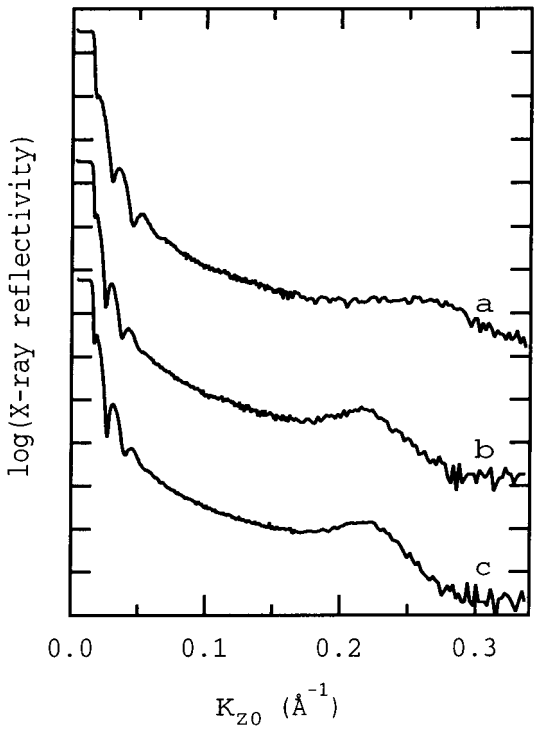

Figure 4. X-ray reflectivity of Si/{**2**/Laponite}$_{10}$ multilayers obtained after different thermal treatments: (a) film heated to 550 °C in air, (b) film heated to 180 °C under vacuum, (c) initial film stored in ambient atmosphere. Measurements were performed in dry argon atmosphere in a closed cell. Curves are displaced vertically for clarity.

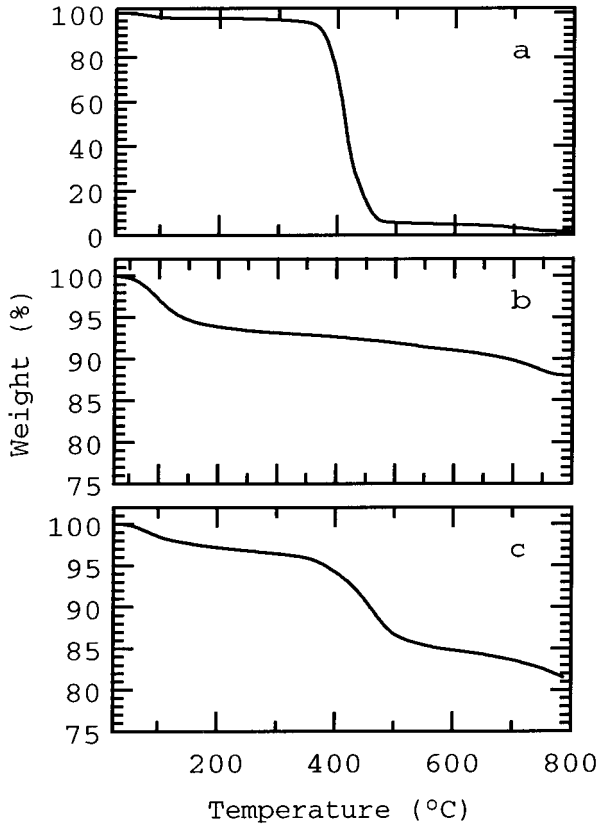

Figure 5. Thermogravimetric analysis of (a) **2**, (b) Laponite powder, and (c) bulk complex (**2**/Laponite) obtained by co-precipitating a solution of **2** with a suspension of Laponite. Measurements were performed in nitrogen atmosphere with a heating rate of 20 °C min^{-1}. Note the different scales for (a)−(c).

Laponite (see below). This variation is attributed to a loss of organic material between the layers of the clay platelets due to pyrolysis.

To improve the understanding of these results, we investigated the thermal behavior of **2** and Laponite. Thermogravimetric analyses (TGA) are presented in Figure 5 (curves a and b). For the clay and **2**, a first slight weight loss occurs between 80 and 110 °C, corresponding to the desorption of bound water. For **2** (curve a), a rapid weight loss beginning approximately at 300 °C marks the thermal decomposition of the polymer into volatile products as previously described.[46] For Laponite (curve b), no weight loss is detected below 700 °C, confirming the thermal stability of the clay in this temperature range. The comparison of these results with the XRR studies indicates that the removal of bound water does not modify significantly the internal structure of the self-assembled films. Moreover, the decrease of the repeat period observed after heating to 550 °C is consistent with the partial pyrolysis of the polycation.

To verify this, we followed by X-ray photoelectron spectroscopy (XPS) the elementary chemical composition of a {**2**/Laponite} multilayer with 10 dipping cycles before and after heating to 550 °C. The experiments were performed at two takeoff angles. Signals of silicon, magnesium, oxygen, carbon, and nitrogen elements were clearly observed. No trace of sodium or bromide counterions could be seen within the detection limit of the technique. The atomic percentages obtained from integration of XPS peaks for different elements are reported in Table 2. The similar values obtained for 30° and 90° takeoff angles imply that the surface contamination of the sample, if any, is so weak than it cannot be detected by XPS. As a consequence, carbon and nitrogen can be safely attributed to the polycation only, whereas silicon, oxygen, and magnesium elements result from the presence of clay in the film. The decrease of carbon content (from 22 to 15%) observed after heating to 550 °C thus reflects the partial pyrolysis of the polymer. Considering that clay platelets are not altered by heating (i.e., the relative amounts of silicon and magnesium remained unchanged), it is possible to estimate the loss of carbon in the sample from the variation of calculated ratios C:Si or C:Mg. This leads to a decrease of carbon content of about 40% upon heating.

Table 2. Atomic Composition (H Excluded) Obtained from XPS (30° and 90° Takeoff Angles) for a Si/{2/Laponite}$_{10}$ Multilayer, before and after Heating to 550 °C

	atomic percentages before heating		atomic percentages after heating to 550 °C	
element	takeoff angle[a] 90°	takeoff angle[a] 30°	takeoff angle[a] 90°	takeoff angle[a] 30°
Si	19	19	24	20
Mg	11	11	13	13
C	22	22	15	17
O	47	46	47	50
N	1	1	0.8	1

[a] With respect to the plane of the surface.

Structure of Bulk Complex (2/Laponite). The mixing of the polycation solution and the clay suspension leads to the formation of an insoluble complex whose internal structure can be compared with the one of self-assembled films for a better understanding of polycation/clay organization.

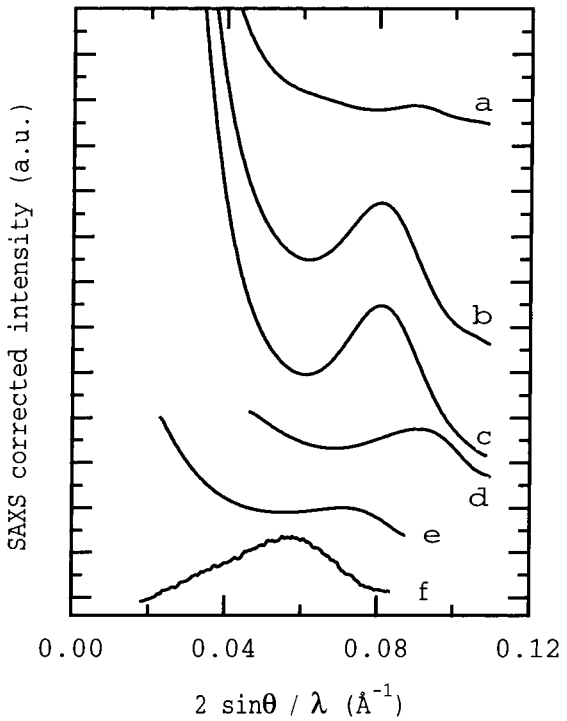

Figure 6. Small-angle X-ray scattering of bulk complex (**2**/Laponite) and Laponite powder obtained after different treatments: bulk complex (a) heated to 550 °C in air, (b) heated to 180 °C under vacuum, (c) stored in ambient atmosphere, and Laponite powder (d) dried to 550 °C in air, (e) stored in ambient atmosphere and (f) stored in moisture atmosphere. Curves are displaced vertically for clarity.

A stoichiometry of 1.2:1 was determined for the (**2**/Laponite) complex by EDX microanalysis (from C, Mg, and Si contents). The slight excess of polycation is hardly significant considering the precision limit of EDX. In addition, no trace of Br counterions could be detected by EDX, indicating the absence of uncomplexed ammonium groups. As a consequence, the real stoichiometry of the complex must be about 1:1.

The internal structure of the complex was investigated by SAXS. A sample conditioned in ambient atmosphere at room temperature was compared with samples obtained after different thermal treatments similar to the ones previously described for multilayers (drying under vacuum at 180 °C for 1 h; heating to 550 °C in ambient atmosphere for 30 min). All measurements, performed in dry helium to avoid moisture, are displayed in Figure 6. Traces obtained for Laponite powder (curves d−f) exposed to various moisture conditions were added in the graph for comparison. The initial complex (curve c) presents an internally ordered structure with a repeat period of 15.2 Å. This value is slightly larger than the one obtained for films prepared with the same polycation (14.4 Å). The difference can be explained by a lower regularity of stacking in the bulk complex. By comparison, the repeat period of Laponite varies from 11 to 17 Å for a dried (curve d) and hydrated (curve f) powder, respectively, showing that the repeat period of the (**2**/Laponite) complex is in the same range as the basal spacing of the hydrated clay sheets. After heating to 550 °C (curve c), the repeat period of the complex decreased to 13.4 Å, in good agreement with the TGA results. This indicates that the polymer decomposes thermally at about 360 °C in the complex into volatile products (Figure 5c). Note that the start of the pyrolysis of **2** is displaced upward by about 60 °C in the complex as compared to free **2** (Figure 5, curves a and c). This behavior was previously reported for other hybrid composites.[56,57] The decomposition of the polymer was confirmed by EDX microanalysis, which showed a net decrease of carbon content after heating of the complex (from 13.7 to 5.5 wt %). In addition, SAXS shows that the repeat period of the heated complex (13.4 Å) is different from the value obtained for dried Laponite (11 Å). This means that the pyrolysis of the polycation intercalated between the inorganic platelets in the complex is incomplete, similar to what was described above for the multilayers. This is confirmed by EDX (5.5 wt % of residual carbon in the heated complex).

Discussion

The fabrication of organized ultrathin films by alternate adsorption of commercial polycations and clay particles was recently reported in the literature.[30−40] In this paper, we extend this procedure to other polycations of various macromolecular structure. An first important result from our study is that no traces of counterions were detected in the multilayer or in the bulk complex by XPS and EDX, respectively. Accordingly, the positive charges of the polycation are balanced by the negative charges of the platelets. This result is in a good agreement with predictions by Schlenoff et al.[3] for {polycation/clay}$_n$ multilayers.

Moreover, all reflectograms of {polycation/Laponite} multilayers present a Bragg peak due to the presence of an ordered structure in the film. Obviously, inorganic platelets diminish interlayer mixing and promote ordering in the multilayers for all polycations used, despite very different chemical structures. Noteworthy, multilayers made from polycation **3** and montmorillonite were studied before in our group.[47] Such multilayers were not found to be ordered as judged from the absence of Bragg peaks in the X-ray reflectograms.[58] The improved order in the {**3**/Laponite} films compared to {**3**/montmorillonite} films is in agreement with the lower roughness reported for adsorbed layers of Laponite compared to montmorillonite.[34]

The repeat period d (14.4 Å) obtained for multilayers {**1**/Laponite}$_n$ is close to the one reported by Kleinfeld and Ferguson[30−33] for the same system (14.5 Å). In addition, **1** and **2** provide the same value of d, consistent with the structural similarity of these polycations. This result also shows that the variation of polycation chain stiffness does not modify the basal spacing. The values of p (thickness of the polymer layer extracted from repeat period d) of 5.2 and 6.5 Å obtained respectively for **1** or **2** and **4** are very small and suggest a very flat conformation of the polycations intercalated between the inorganic platelets. The comparison of XRR results obtained for all samples studied suggests that the structure of the polycation slightly modulates the spatial extent of order in the film as well as the value of the repeat period. The latter seems to increase with the volume per charge of macromolecule (Table 1).

Density profiles and Patterson functions obtained for different {polycation/Laponite}$_n$ multilayers show that a damping of order occurs further away from the substrate. The damping of order is due either to increasing misorientation of the platelets vs substrate surface as distance from substrate increases or to a random staggering of each platelet vs its lateral neighbors. The observation that the basal spacing d (XRR)

and the increment of growth (ellipsometry) are different indicates that multilayer buildup does not proceed by simple deposition of monolayers of clay and polymer at each deposition step. A similar behavior was reported for {PDDA/Laponite}$_n$[30−33] and {PDDA/montmorillonite}$_n$[37] multilayers. Importantly, this complex film growth is not specific to these {polycation/clay}$_n$ multilayers but was reported for other layer-by-layer polyelectrolyte self-assemblies,[6] too.

In the literature, different models were proposed to describe the internal structure of {polycation/clay} multilayers. Kotov and co-workers[37] suggested that the Bragg peak observed for multilayers prepared with natural clay only results from the presence of unexfoliated stacks of clay platelets. Defects due to nonexfoliated platelets were clearly shown on the surface of films by atomic force microscopy.[34,37] However, this interpretation is not valid in our case considering the combined results of the XPS, XRR, and TGA studies for the sample {**2**/Laponite}$_n$. The variation of the repeat distance and the chemical composition of the film upon heating proves that the polycation is intercalated between exfoliated inorganic platelets and is not in agreement with the dehydration of undelaminated stacks of clay platelets as suggested in the past.[37] Moreover, the analysis of the bulk (**2**/Laponite) complex which presents a structure similar to the film supports this conclusion. So, sheets of Laponite are adsorbed as individual particles during the deposition process (which could be different for natural clays). Such possible difference could be explained by the smaller size of platelets and the lower crystallinity of synthetic Laponite compared with natural clays like montmorillonite or hectorite, allowing for easier exfoliation.

Conclusion

By combining XRR, TGA, and XPS measurements, we demonstrated that the internal order present in multilayers of {polycations/clay} is due to a regular structure resulting from the intercalation of polycation between exfoliated clay platelets. This conclusion is corroborated by the analysis of the bulk (polycation/clay) complex by SAXS, TGA, and EDX. Importantly, the chemical analysis of (polycation/clay) systems (multilayer or complex) shows the absence of low molar mass counterions. This result demonstrates a full charge compensation between the polycations and the negatively charged clay platelets.

Finally, for all polycations used, we showed that the large scale order in the self-assembled film is limited to the first deposited layers. The structure of the polycation does not strongly influence the spatial extent of order or the value of the repeat period. In a future paper, we will report in detail on the film growth process to improve our current understanding of the loss of internal order with distance from substrate.

Acknowledgment. The authors thank E. Wischerhoff and P. Fischer for their contributions to the synthesis of the polycations as well as A. S. Duwez and J. Ghijsen (LISE, FUNDP; Namur, Belgium) for the XPS measurements and R. Morlat for his help in EDX measurements. The research was financially supported by the DG Recherche Scientifique of the French Community of Belgium (Actions de Recherches Concertées 94/99-173 and 00/05-261) and by the Belgian National Fund for Scientific Research.

References and Notes

(1) Decher, G. *Science* **1997**, *277*, 1232.
(2) Arys, X.; Jonas, A. M.; Laschewsky, A.; Legras, R. In *Supramolecular Polymers;* Ciferri, A., Ed.; Marcel Dekker: New York, 2000; p 505.
(3) Schlenoff, J. B.; Ly, H.; Li, M. *J. Am. Chem. Soc.* **1998**, *120*, 7626.
(4) Farhat, T.; Yassin, G.; Dubas, S. T.; Schlenoff, J. B. *Langmuir* **1999**, *15*, 6621.
(5) Rubner, M. *Proc. Am. Chem. Soc. Div. Polym. Mater. Sci. Eng.* **2000**, *83*, 554.
(6) Arys, A.; Laschewsky, A.; Jonas, A. M. *Macromolecules*, in press.
(7) Fang, M.; Kim, C. H.; Saupe, G. B.; Kim, H.-N.; Waraksa, C. C.; Miwa, T.; Fujishima, A.; Mallouk, T. E. *Chem. Mater.* **1999**, *11*, 1526.
(8) Kimizuka, N.; Tanaka, M.; Kunitake, T. *Chem. Lett.* **1999**, 1333.
(9) Sasaki, T.; Ebina, Y.; Watanabe, M.; Decher, G. *Chem. Commun.* **2000**, 2163.
(10) Keller, S. W.; Kim, H.-N.; Mallouk, T. E. *J. Am. Chem. Soc.* **1994**, *116*, 8817.
(11) Kaschak, D. M.; Mallouk, T. E. *J. Am. Chem. Soc.* **1996**, *118*, 4222.
(12) Feldheim, D. L.; Grabar, K. C.; Natan, M. J.; Mallouk, T. E. *J. Am. Chem. Soc.* **1996**, *118*, 7640.
(13) Fang, M.; Kaschak, D. M.; Sutorik, A. C.; Mallouk, T. E. *J. Am. Chem. Soc.* **1997**, *119*, 12184.
(14) Kim, H.-N.; Keller, S. W.; Mallouk, T. E. *Chem. Mater.* **1997**, *9*, 1414.
(15) Kerimo, J.; Adams, D. M.; Barbara, P. F.; Kaschak, D. M.; Mallouk, T. E. *J. Phys. Chem. B* **1998**, *102*, 9451.
(16) Kaschak, D. M.; Lean, J. T.; Waraksa, C. C.; Saupe, G. B.; Usami, H.; Mallouk, T. E. *J. Am. Chem. Soc* **1999**, *121*, 3435.
(17) Kaschak, D. M.; Johnson, S. A.; Waraksa, C. C.; Pogue, J.; Mallouk, T. E. *Coord. Chem. Rev.* **1999**, *185−186*, 403.
(18) Ollivier, P. J.; Kovtyukhova, N. I.; Keller, S. W.; Mallouk, T. E. *Chem. Commun.* **1998**, 1563.
(19) Fendler, J. H. *Chem. Mater.* **1996**, *8*, 1616.
(20) Ingersoll, D.; Kulesza, P. J.; Faulkner, L. R. *J. Electrochem. Soc.* **1994**, *141*, 140.
(21) Ichinose, I.; Tagawa, H.; Mizuki, S.; Lvov, Y.; Kunitake, T. *Langmuir* **1998**, *14*, 187.
(22) Moriguchi, I.; Fendler, J. H. *Chem. Mater.* **1998**, *10*, 2205.
(23) Caruso, F.; Kurth, D. G.; Volkmer, D.; Koop, M. J.; Muller, A. *Langmuir* **1998**, *14*, 3462.
(24) Kovtyukhova, N. I.; Ollivier, P. J.; Martin, B. R.; Mallouk, T. E.; Chizhik, S. A.; Buzaneva, E. V.; Gorchinskiy, A. D. *Chem. Mater.* **1999**, *11*, 771.
(25) Cassagneau, T.; Fendler, J. H. *J. Phys. Chem. B* **1999**, *103*, 1789.
(26) Cassagneau, T.; Fendler, J. H. *Adv. Mater.* **1998**, *10*, 877.
(27) Kotov, N. A.; Dékany, I.; Fendler, J. H. *Adv. Mater.* **1996**, *8*, 637.
(28) Cassagneau, T.; Guérin, F.; Fendler, J. H. *Langmuir* **2000**, *16*, 7318.
(29) Schaak, R. E.; Mallouk, T. E. *Chem. Mater.* **2000**, *12*, 2513.
(30) Kleinfeld, E. R.; Ferguson, G. S. *Science* **1994**, *265*, 370.
(31) Kleinfeld, E. R.; Ferguson, G. S. *Chem. Mater.* **1995**, *7*, 2327.
(32) Kleinfeld, E. R.; Ferguson, G. S. *Chem. Mater.* **1996**, *8*, 1575.
(33) Ferguson, G. S.; Kleinfeld, E. R. *Adv. Mater.* **1995**, *7*, 414.
(34) van Duffel, B.; Schoonheydt, R. A.; Grim, C. P. M.; De Schryver, F. C. *Langmuir* **1999**, *15*, 7520.
(35) Lvov, Y.; Ariga, K.; Ichinose, I.; Kunitake, T. *Langmuir* **1996**, *12*, 3038.
(36) Lvov, Y.; Ariga, K.; Ichinose, I.; Kunitake, T. *Thin Solid Films* **1996**, *284−285*, 797.
(37) Kotov, N. A.; Haraszti, T.; Turi, L.; Zavala, G.; Geer, R. E.; Dékány, I.; Fendler, J. H. *J. Am. Chem. Soc.* **1997**, *119*, 6821.
(38) Kotov, N. A.; Magonov, S.; Tropsha, E. *Chem. Mater.* **1998**, *10*, 886.
(39) Rouse, J. H.; MacNeill, B. A.; Ferguson, G. S. *Chem. Mater.* **2000**, *12*, 2502.
(40) Mamedov, A.; Ostrander, J.; Aliev, F.; Kotov, N. A. *Langmuir* **2000**, *16*, 3941.
(41) Durand-Piana, G.; Lafuma, F.; Audebert, R. *J. Colloid Interface Sci.* **1987**, *119*, 474.
(42) Arys, X. Understanding Ordering in Polyelectrolyte Multilayers: Effect of the Chemical Architecture of the Polycation. PhD Dissertation, Université catholique de Louvain, Louvain-la-Neuve, Belgium, 2000.
(43) Laschewsky, A.; Zerbe, I. *Polymer* **1991**, *32*, 2089.

(44) Dautzenberg, H.; Jaeger, W.; Kötz, J.; Philipp, B.; Seidel, C.; Stscherbina, D. In *Polyelectrolytes: Formation, Characterization and Application*; Hanser: Munich, 1994; p 11.
(45) Schlenoff, J. B.; Dubas, S. T. *Macromolecules* **2001**, *34*, 592.
(46) De Vynck, V.; Goethals, E. J. *Macromol. Rapid Commun.* **1997**, *18*, 149.
(47) Laschewsky, A.; Wischerhoff, E.; Kauranen, M.; Persoons, A. *Macromolecules* **1997**, *30*, 8304.
(48) Köberle, P.; Laschewsky, A.; van den Boogaard, D. *Polymer* **1992**, *33*, 4029.
(49) Laschewsky, A.; Zerbe, I. *Polymer* **1991**, *32*, 2070.
(50) Kleim, R.; Kuntzler, L.; El Ghemmaz, A. J. *J. Opt. Soc. Am. A* **1994**, *11*, 2550.
(51) Azzam, R. M. A.; Bashara, N. M. *Ellipsometry and Polarized Light;* North-Holland: Amsterdam, 1997.
(52) Aspnes, D. E.; Studna, A. A. *Phys. Rev. B* **1983**, *27*, 985.
(53) Whelan, C. M.; Barnes, C. J.; Walker, C. G. H.; Brown, N. M. D. *Surf. Sci.* **1999**, *425*, 195.
(54) Whelan, C. M.; Smyth, M. R.; Barnes, C. J. *Langmuir* **1999**, *15*, 116.
(55) Ladam, G.; Schaad, P.; Voegel, J. C.; Schaaf, P.; Decher, G.; Cuisinier, F. *Langmuir* **2000**, *16*, 1249.
(56) Kioul, A.; Mascia, L. *J. Non-Cryst. Solids* **1994**, *175*, 169.
(57) Mauritz, K. A.; Jones, C. K. *J. Appl. Polym. Sci.* **1990**, *40*, 1401.
(58) Fisher, P.; Jonas, A. M.; Laschewsky, A.; Wischerhoff, E., unpublished results.

MA010123J